

Ralf Weisse · Heinz Günther

Wave climate and long-term changes for the Southern North Sea obtained from a high-resolution hindcast 1958–2002

Received: 16 June 2006 / Accepted: 15 November 2006 / Published online: 24 January 2007
© Springer-Verlag 2007

Abstract An analysis of the extreme wave conditions in 1958–2002 in the North Sea as obtained from a regional model hindcast is presented. The model was driven by hourly wind fields obtained from a regional atmosphere model forced with reanalysis data from the National Center for Environmental Prediction (NCEP/NCAR). Furthermore, observed sea ice conditions from the Norwegian Meteorological Institute have been accounted for in the simulation. It is shown that the model is capable of reproducing extreme wave height statistics at a reasonable degree of approximation. The analysis of severe wave height events reveals that for much of the Southern North Sea, their number has increased since the beginning of the simulation period (1958), although the increase has attenuated later and leveled off around about 1985. On the other hand, the intensity and duration of severe wave height events decreased within the last few years of the simulation so that annual 99%-ile wave heights have also reduced since about 1990–1995. For the UK North Sea coast, a different behavior was found characterized by a reduction in severe wave conditions over much of the hindcast period.

Keywords Waves · Wave climate · Sea state · Long-term changes · Climate variability · North Sea

1 Introduction

At sea, storms and wind waves generated by these storms (the sea state) represent major threats for human activities such as commercial shipping, offshore activities, and coastal defense. To cope with the hazards associated with heavy sea states, extreme event statistics are needed, which

in turn require homogeneous and long observational records. Unfortunately, such data are hardly available. In particular for sea states, in many cases, the records are limited to some observations for more or less limited periods from a more or less nearby measurement site. In some cases, these data may be complemented with even shorter and less frequent data from satellite instruments. Hindcasts with ocean wave models have therefore become a common tool to complement the limited observational record. Usually, such hindcasts are validated with the limited observational material available and are later regarded as a reality substitute from which information can be drawn on variables that have either not been measured directly or which have been sampled only insufficiently in space and time.

At the beginning, such wave hindcasts have generally been performed for short periods of time such as a few months or for individual storm events only (e.g., Ewing et al. 1979; Cardone et al. 1996). Apart from some undisclosed studies, the first comprehensive public attempt to hindcast several decades of years has, to our knowledge, been provided by The WASA-Group (1998). By applying an as homogeneous as possible wind field to drive their wave model with, for the first time, an ocean wave hindcast became available from which extreme event statistics as well as their long-term changes could be assessed. Details of this effort are described in Günther et al. (1998). Later, similar attempts have been made for the globe (e.g., Sterl et al. 1998; Cox and Swail 2001) or for different ocean basins (e.g., Wang and Swail 2002). Recently, a global wave hindcast has also been produced within the ERA-40 reanalysis project (Sterl and Caires 2005; Caires and Sterl 2005).

Today, there exist a number of multi-decadal hindcasts that cover the globe or at least large parts of the major ocean basins such as the Atlantic or Pacific Ocean. Human activities, however, mostly require information on the local scale and/or near the coasts. For instance, the North Sea, which is surrounded by densely populated and highly industrialized countries, is hardly covered by these hindcasts. Large areas along the North Sea coast are

Responsible editor: Roger Proctor

R. Weisse (✉) · H. Günther
Institute for Coastal Research, GKSS Research Center,
Max-Planck-Str. 1,
21502 Geesthacht, Germany
e-mail: weisse@gkss.de

below or only slightly above mean sea level, and enormous efforts to protect these areas are made every year. In addition, the North Sea is one of the most frequently traversed sea areas, and some of the busiest shipping routes in the world are found in the North Sea. For example, in 1996, about 270,000 ships were entering the 50 major ports in the area (OSPAR Commission 2000). Since the late 1960s, offshore oil and gas industry has become a major economic activity with the number of platforms increasing by almost 60% within one decade (1990–1992/1996–1998; OSPAR Commission 2000).

In this paper, we present a multi-decadal (1958–2002) high-resolution wave hindcast for the Southern North Sea. The hindcast has been carried out as part of an effort to provide a consistent met-ocean hindcast for the area consisting of high-resolution wind fields (Feser et al. 2001; Weisse et al. 2005), high-resolution tide-surge levels and currents (Weisse and Pluess 2006), and the above mentioned high-resolution ocean wave hindcast. The paper is structured as follows. In Section 2, the met-ocean hindcast, with emphasis on the ocean wave part, is briefly described. In Section 3, the hindcast is compared and validated with observational wind and wave data. The reconstructed (hindcast) wave climate is described in Section 4 with emphasis on extreme wave conditions. Long-term variability and trends in extreme sea state

conditions are elaborated in Section 5. In Section 6, our results are summarized and discussed.

2 The 1958–2002 North Sea wave hindcast

A spatially and temporal high-resolution wave hindcast for the Southern North Sea has been provided as part of a consistent met-ocean hindcast for the area. The met-ocean hindcast consists of an atmospheric reconstruction with a regional atmosphere model (Feser et al. 2001) driven by the NCEP/NCAR weather reanalyzes (Kalnay et al. 1996; Kistler et al. 2001), a tide-surge hindcast driven by these reconstructed wind fields (Weisse and Pluess 2006), and the ocean wave hindcast described in this paper (Fig. 1).

For the wave hindcast, the wave model WAM (The WAMDI-Group 1988) was set-up in a nested version with a coarse grid covering the entire North Sea and large parts of the Northeastern North Atlantic and a fine grid covering the North Sea south of 56°S (Southern North Sea). The spatial resolutions were about 50×50 and 5.5×5.5 km for the coarse and the fine grid respectively. For both grids, wave spectra were computed with a directional discretization of 15° and at 28 frequencies ranging non-linearly from about 0.042 to 0.55 Hz. The latter corresponds to wavelengths between about 5 and 900 m. For the fine grid, the wave

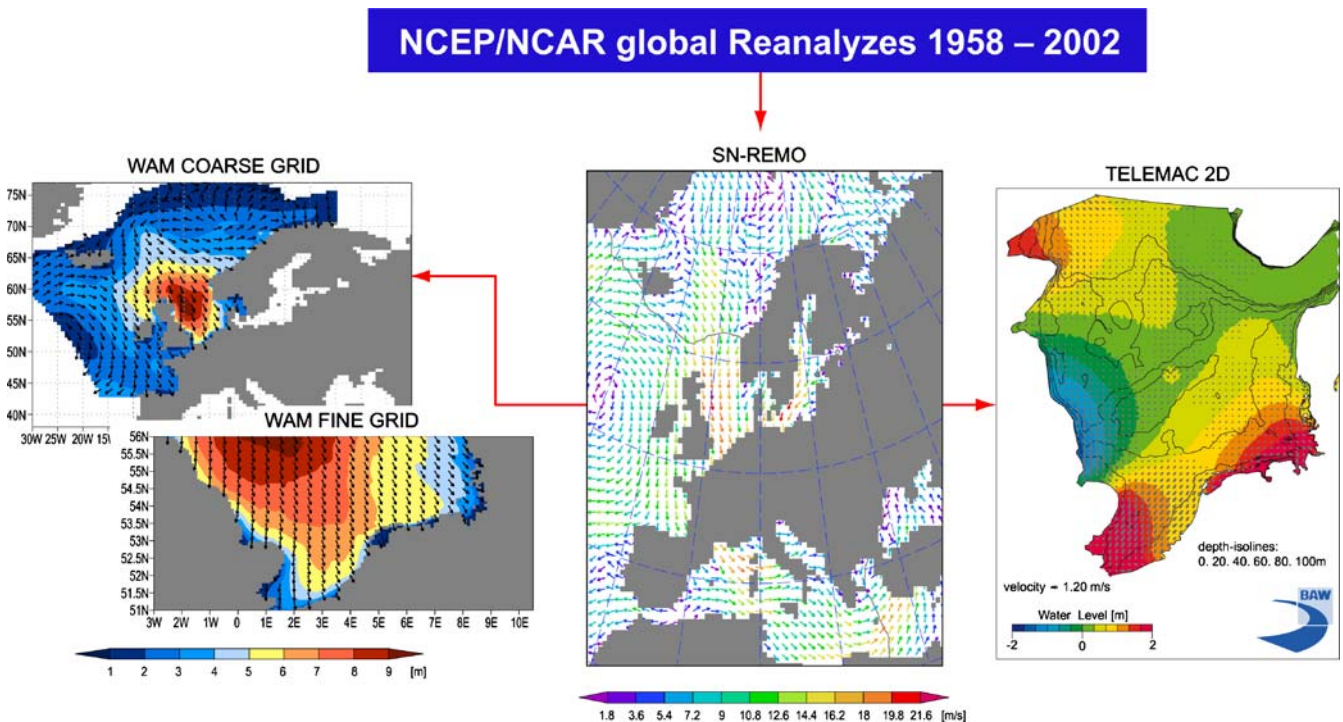


Fig. 1 Layout of the consistent met-ocean hindcast 1958–2002 for the Southern North Sea. From the regional atmosphere hindcast (*middle*), hourly wind fields were used to force a tide-surge (*right*) and a wave model hindcast (*left*). The tide-surge model was integrated on an unstructured grid with typical resolutions of about 5–10 km in the open North Sea and about 100 m near the coast and the estuaries. The figure shows an example of consistent met-ocean conditions obtained from the hindcast for 12 UTC on 21 February

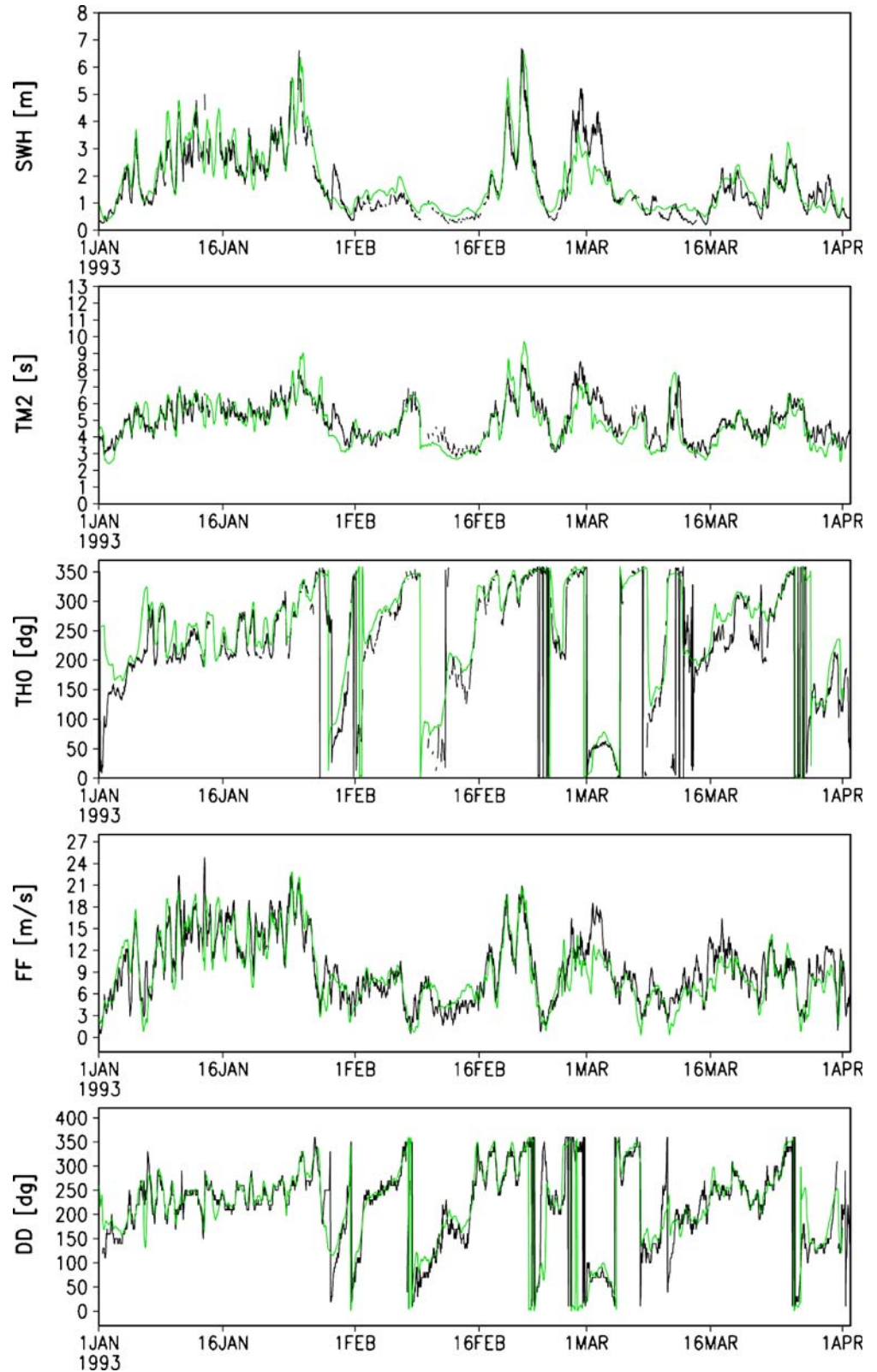
1993. *Middle* Near-surface (10-m height) marine wind fields in ms^{-1} and corresponding wind direction obtained from the regional atmospheric reconstruction. *Left* Corresponding significant wave height fields in m and mean wave direction from the coarse and the fine grid wave model hindcast. *Right* Tide-surge levels in m from the corresponding tide-surge hindcast. The tide-surge and wave hindcasts were performed as part of the HIPOCAS project (Soares et al. 2002)

model was run in shallow water mode, whereas for the coarse grid observed sea ice conditions from the Norwegian Meteorological Institute have been taken into account.

The wind fields used to drive the wave model with represent an integral part of the consistent met-ocean

hindcast for the Southern North Sea. They were obtained from the aforementioned 1958–2002 regional atmospheric reconstruction (Feser et al. 2001) using the regional atmosphere model REMO (Jacob and Podzun 1997) driven by the NCEP/NCAR weather reanalysis (Kalnay et al.

Fig. 2 Time series of significant wave height [m], TM2 wave period [s], mean wave direction [degrees coming from], wind speed [ms^{-1}] and wind direction [degrees coming from] (from *top to bottom*) at K13 for a 3-month period 01 January 1993–31 March 1993. Observations, *black*; model results, *green*



1996; Kistler et al. 2001) for the same period (Fig. 1). The model was run in combination with a spectral nudging method, which in the absence of observations not assimilated in the driving reanalysis, may be considered as a simple data assimilation procedure (von Storch et al. 2000). In this set-up the REMO model is usually referred to as SN-REMO (Meinke et al. 2004). The SN-REMO model was run at a spatial resolution of about 50×50 km driven by 6-hourly boundary data from the NCEP/NCAR weather reanalysis. The latter have a spatial resolution of about 210×210 km. Near-surface wind fields from the SN-REMO hindcast are available for each hour within the period 1958–2002 and have been bilinearly interpolated in space to the wave model resolution.

The wave model was integrated for the period 1958–2002. For the fine grid, two-dimensional wave spectra have been stored every 3 h, whereas integrated wave parameters such as significant wave height, mean wave direction, and different wave periods are available every hour.

In the next section, we assess the extent to which the 1958–2002 wave hindcast is capable of reproducing observed conditions. The quality of wind fields has been evaluated by von Storch et al. (2000), Weisse and Feser (2003), and Weisse et al. (2005). In the latter, special emphasis was given on extreme events, i.e., the storm climate and its long-term fluctuations. It was found that the

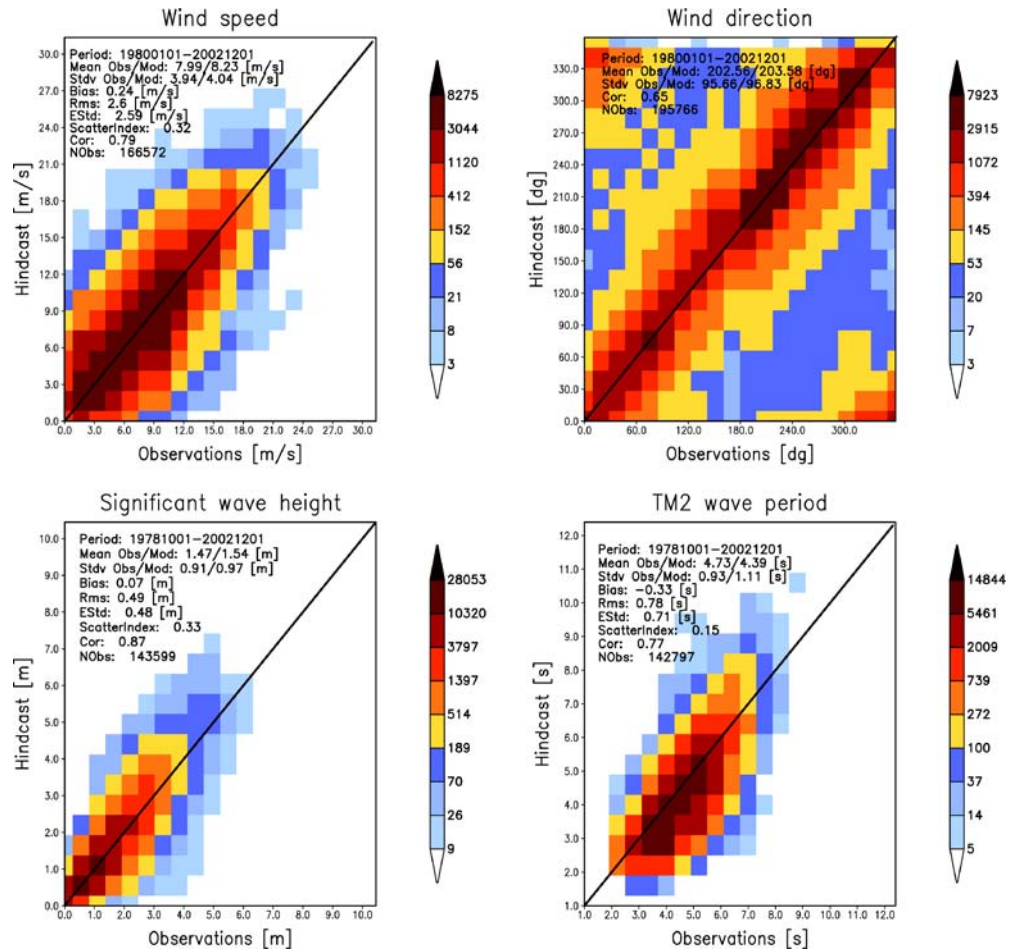
SN-REMO hindcast provides a reasonable description of the recent Northeast Atlantic and North Sea storm climate and its variability. The quality of the tide-surge hindcast has been assessed in detail in Weisse and Pluess (2006). Again, it was concluded that the tide-surge climate is reasonably reproduced within the hindcast period.

3 Validation

In the following, we investigate the extent to which the wave hindcast reproduces observed conditions. Figure 2 shows a comparison between observed and hindcast wind speed and direction as well as significant wave height, period, and wave direction for a 3 months period at station K13 (53.22°N , 3.22°E). In principal, a good agreement can be inferred. For instance, the storm event on 21 February, which caused observed significant wave heights of more than 6 m, is reasonably reproduced for all parameters. On the other hand, there are also events with larger discrepancies such as the one-around 1 March for which wave heights are considerably underestimated, in this case caused by too low wind speeds in the atmospheric hindcast (Fig. 2).

A comparison for the entire period for which observations were available at K13 is presented in Fig. 3. For wind

Fig. 3 Scatterplot between observed (x-axis) and hindcast (y-axis) hourly wind speeds in ms^{-1} (upper left), wind direction in degrees coming from (upper right), significant wave height in m (lower left), and TM2 wave period in s (lower right) at K13. Colors indicate the number of cases in each class. In addition, the following statistics are presented (from top): Analysis period, observation and hindcast mean, observation and hindcast standard deviation, bias and root-mean-square error between observations and hindcast, standard deviation of the differences between hindcast and observations, scatter index, correlation, and number of observed/hindcast data values that have been used in the analysis



speed, very little bias can be inferred, and the frequencies with which severe events are over- or underestimated are essentially the same. The latter indicates that although individual storms may or may not be captured by the hindcast, their statistics remain unbiased, and the hindcast may be used as substitute reality to study the statistics of extreme events and their long-term variability. A similar conclusion holds for wind direction and significant wave height, although some tendency to overestimate the most extreme wave periods can be inferred.

A similar comparison was made for some more stations. The error statistics for four of them are listed in Table 1. For Europlatform (EUR) located at a water depth comparable to that of K13 (more than 20 m), similar conclusions as for K13 do hold. For Schiermonnikoog (SON), which is located in 19-m water depth surrounded by shoals, and Huibertgat (HBG; land station), differences between observations and hindcast are somewhat larger.

To investigate in particular the extent to which extreme value statistics are reproduced, we analyzed and compared return values derived from hindcast and observed data (Table 2). For wind speed, the estimated return values agree well within the 90%-confidence limit estimated from

Monte Carlo simulations. A similar conclusion holds for the significant wave height at K13 and EUR, although hindcast return values systematically appear to be above the observed ones. For SON surrounded by rather shallow water, hindcast return values are significantly different from the observed ones with the hindcast overestimating observations. The latter may be partially explained by the 5.5×5.5 km resolution of the wave model in which the shoals surrounding SON are not very well resolved.

Summarizing, it was found that the wave hindcast reasonably reproduces observed extreme value statistics except for stations with complex topographic features, which are not well represented at the spatial resolution the hindcast was made at. In our set-up, this typically results in reasonable hindcast statistics seaward of about 10–15 m water depth. Gaslikova and Weisse (2006) have demonstrated, however, that the ocean wave hindcast described in this paper still provides reasonable boundary conditions for very shallow water wave modeling and that a better representation of near-shore wave conditions can be obtained when further downscaling is applied. We therefore suggest that our wave hindcast may be used directly for analyzing extreme wave statistics seaward of about 10–15 m water depth, whereas for shallower locations additional simulations with a shallow water wave model using our hindcast as boundary conditions may be performed.

Table 1 Comparison between observations and hindcast at K13, EUR, HBG, and SON

Station	Position	\bar{x}_o	\bar{x}_h	b	r	c
Wind speed [ms^{-1}]						
K13	53.22°N 03.22°E	7.99	8.23	0.24	2.60	0.79
EUR	52.00°N 03.28°E	7.90	7.52	-0.38	2.33	0.82
HBG	53.57°N 06.40°E	7.90	7.64	-0.26	3.14	0.66
SON	53.60°N 06.17°E	N.A.	N.A.	N.A.	N.A.	N.A.
Significant wave height [m]						
K13	53.22°N 03.22°E	1.47	1.54	0.07	0.49	0.87
EUR	52.00°N 03.28°E	1.26	1.21	-0.05	0.41	0.87
HBG	53.57°N 06.40°E	N.A.	N.A.	N.A.	N.A.	N.A.
SON	53.60°N 06.17°E	1.26	1.19	-0.07	0.63	0.70

\bar{x}_o : observation mean, \bar{x}_h : hindcast mean, b : bias, r : root-mean-square error, c : correlation

Upper part, wind speed; lower part, total significant wave height. The statistics have been computed for the periods for which observational data have been available, in particular at K13 from October 1978 to December 2002 and from January 1980 to December 2002 for waves and wind respectively, at EUR from January 1983 to December 2002, at HBG from January 1981 to December 2000, and at SON from December 1979 to October 2000.

4 Hindcast wave climate 1958–2002

In the following, the hindcast wave climate representative for the period 1958–2002 is presented for the Southern North Sea. As severe wave conditions have the largest implications for many sectors such as coastal protection, shipping, or offshore constructions, the analysis is limited to extreme wave conditions. We concentrate on the local long-term (1958–2002) 99%-ile of total significant wave height as a threshold to determine severe wave conditions. For hourly values, this threshold, on average, is exceeded for 3–4 days a year. In the following, we refer to this threshold as the *severe event threshold* (SET). Based on the SET, we define the following parameters

- The *number of extreme events* represents the annual number of exceedances of the SET.
- The *average duration* of these events is given by the annual time for which the significant wave height remains above the SET divided by the number of events within the same year.
- The *mean intensity* of extreme events is given by the average intensity of all individual events within 1 year, where the intensity of an event is defined as the difference between the maximum significant wave height that occurred during the event and the SET.

Figure 4 illustrates the definition of these parameters in the following referred to as exceedance statistics.

The severe wave event climate for the Southern North Sea 1958–2002 as obtained from the wave hindcast is

Table 2 Comparison of 2, 5, and 25-year return values (x_r) estimated from observed and hindcast wind speed and significant wave height at K13, EUR, HBG, and SON

		Wind speed [ms^{-1}]						Significant wave height [m]					
		Hindcast			Observations			Hindcast			Observations		
	$T[\text{yr}]$	$x_r^{90} \leq$	x_r	$\leq x_r^{90}$	$x_r^{90} \leq$	x_r	$\leq x_r^{90}$	$x_r^{90} \leq$	x_r	$\leq x_r^{90}$	$x_r^{90} \leq$	x_r	$\leq x_r^{90}$
K13	2	24.4	25.2	26.0	24.1	25.2	26.4	7.1	7.5	7.9	6.4	6.8	7.1
	5	25.9	27.3	28.7	25.8	27.6	29.5	7.8	8.4	9.0	6.9	7.5	8.2
	25	28.4	31.3	34.2	28.1	32.8	37.5	9.0	10.4	11.7	7.5	9.2	10.9
EUR	2	22.5	23.2	23.8	23.2	24.0	24.9	5.9	6.2	6.4	5.5	5.8	6.2
	5	23.8	24.8	25.9	24.3	25.9	27.6	6.3	6.8	7.3	5.9	6.5	7.0
	25	25.7	28.0	30.3	26.4	29.8	33.1	6.9	8.2	9.5	6.0	7.9	9.8
HBG	2	23.3	24.2	25.0	23.1	24.0	25.0	N.A.	N.A.	N.A.	N.A.	N.A.	N.A.
	5	24.9	26.3	27.8	24.2	26.0	27.7	N.A.	N.A.	N.A.	N.A.	N.A.	N.A.
	25	26.7	30.7	34.7	26.4	29.8	33.1	N.A.	N.A.	N.A.	N.A.	N.A.	N.A.
SON	2	N.A.	N.A.	N.A.	N.A.	N.A.	N.A.	6.8	7.1	7.3	5.6	5.8	6.1
	5	N.A.	N.A.	N.A.	N.A.	N.A.	N.A.	7.4	7.8	8.2	6.0	6.5	7.0
	25	N.A.	N.A.	N.A.	N.A.	N.A.	N.A.	8.0	9.0	10.0	6.3	7.9	9.4

Additionally shown is the 90% confidence interval x_r^{90} obtained from 1,000 Monte Carlo simulations each. T denotes the return periods

shown in Fig. 5. It can be inferred that the 99%-ile significant wave height (SET) is generally largest toward the north of the model domain where it reaches values of up to 6.5 m. Toward the south and toward the coasts, the long-term 99%-ile wave height generally decreases, reaching values of about 4–5 m in the German Bight and off the coasts. For large parts of the Southern North Sea, typical values of about 5–6 m are found.

For most parts of the Southern North Sea, the SET is exceeded on an average of 8–9 times a year. An exception is provided by parts of the UK coast where extreme events occur a little less frequent. Once the significant wave height

is above the SET, it remains there on average for about 10–11 h for large parts of the Southern North Sea. Again, an exception is found for the UK coast where the duration of the events is somewhat longer. Typical intensities of the events vary between about 0.8–1.3 m above the SET.

For each event exceeding the local SET, we determined a characteristic T_{m2} -period and mean wave direction. Considering all extreme events in 1958–2002, the most frequent characteristic T_{m2} -period and mean wave direction are shown in Fig. 6. It can be inferred that severe waves in the Southern North Sea typically have periods of about 8–9 s. Off the UK coasts, periods typically range from 7–8 s, whereas even smaller periods are found close to the English Channel. In the eastern part, severe wave events most frequently approach from westerly to north-westerly directions. In the western part, severe events more typically arrive from northwesterly or northerly directions. Along a small stripe at the UK coast, severe wave events are usually approaching from easterly directions. This behavior can be associated with the typical eastward path of mid-latitude cyclones and the sheltering effect of the UK land mass.

So far, we have provided a description of extreme wave climate characteristics from the wave hindcast. They should be considered as an analysis example as there are many more different aspects possible to consider. The latter usually depends on application, and it is not possible to outline the full spectrum of wave climate information inherent in the wave hindcast. Further examples may be obtained for instance from Weisse et al. (2003) or the Hindcast of Dynamic Processes of the Oceans and the Coastal Areas of Europe (HIPOCAS) North Sea Atlas webpage (http://www.gkss.de/pages.php?page=k_ksa_atlas.html&language=e&version=g).

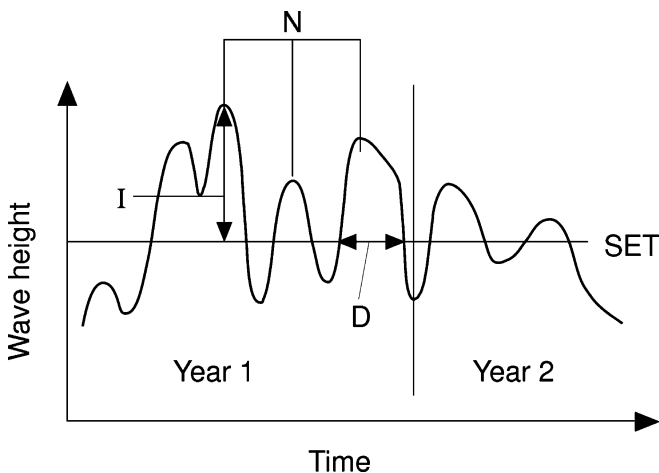


Fig. 4 Definition of parameters that characterize extreme wave event statistics. Here, SET denotes the severe event threshold, N the annual number of extreme events, D their duration, and I the intensity of these events

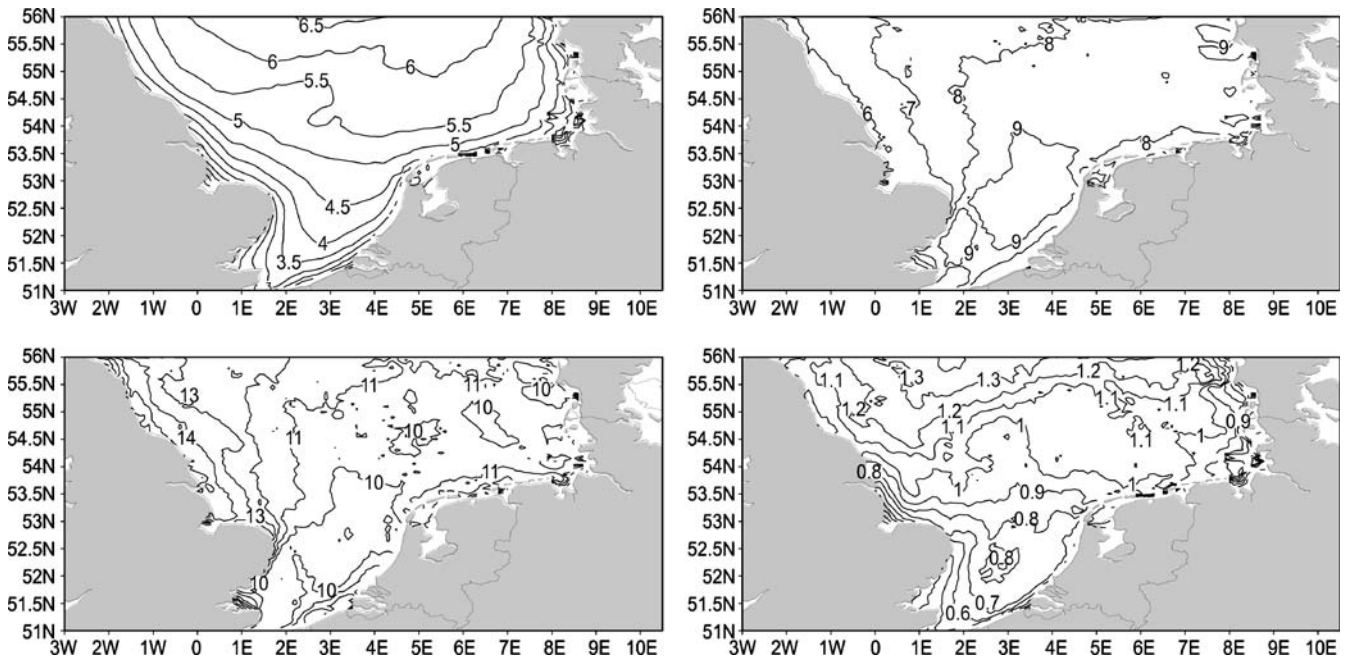


Fig. 5 Long-term 1958–2002 99%-ile of total significant wave height in m (SET, upper left), the average number of events per year exceeding the SET (upper right), the average duration in h (lower left), and the average intensity in m (lower right) of these events

5 Long-term variability and trends

So far, we have described the mean extreme wave climate of the wave hindcast. In the following, we concentrate

on its long-term variability and trends and how they relate to the documented changes in North Sea storminess.

Figure 7 shows the linear trends in 1958–2002 for different severe wave event characteristics. It can be obtained that the annual 99%-ile wave height has increased off The Netherlands, the German, and the Danish coasts with a maximum of up to 1.8 cm year^{-1} off the East Frisian coast. The latter corresponds to about 80 cm in 45 years or about 15% of the long-term 99%-ile wave height. Off the UK coast, decreasing extreme wave heights of up to 0.6 cm year^{-1} are found for some areas. It can be inferred that the increase in the 99%-ile wave heights in the southeastern part of the model domain is mainly caused by an increase in the number of extreme events, whereas their duration and intensity revealed no significant changes (Fig. 7). The number of extreme events has increased at a rate of about 0.15 every year corresponding to almost seven events per year over the entire hindcast period. Contrary to the continental coasts, the changes along the UK coast are not caused by significant changes in the number of severe events. Here, the latter remained relatively unchanged, whereas the average duration of extreme events exhibits a significant negative trend of up to 6 min year^{-1} , which is probably caused by changes in the prevailing directions the waves are coming from. The different causes of the described changes in extreme wave climate may have different implications for different applications. For example, dikes and levees are likely to be more sensitive to the duration than to the number of impacts, whereas for the operation of a ferry route, the number of days with no or only restricted services because of heavy seas may be an issue.

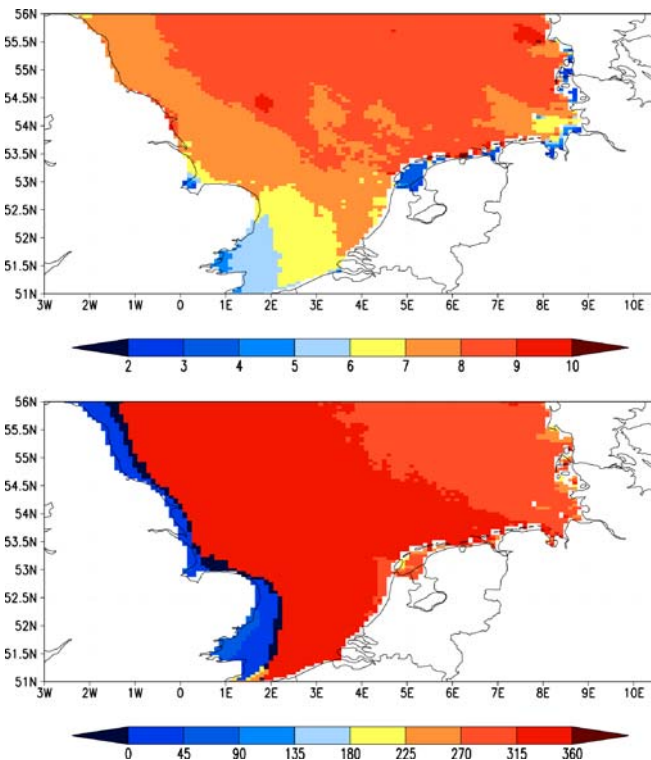


Fig. 6 Most frequent Tm2-period in s (top) and most frequent mean wave direction in degrees coming from (bottom) associated with severe wave events 1958–2002

As a next step, we investigate the extent to which the above described trends are characteristic for the entire 1958–2002 hindcast period. From the analysis of long-term storm

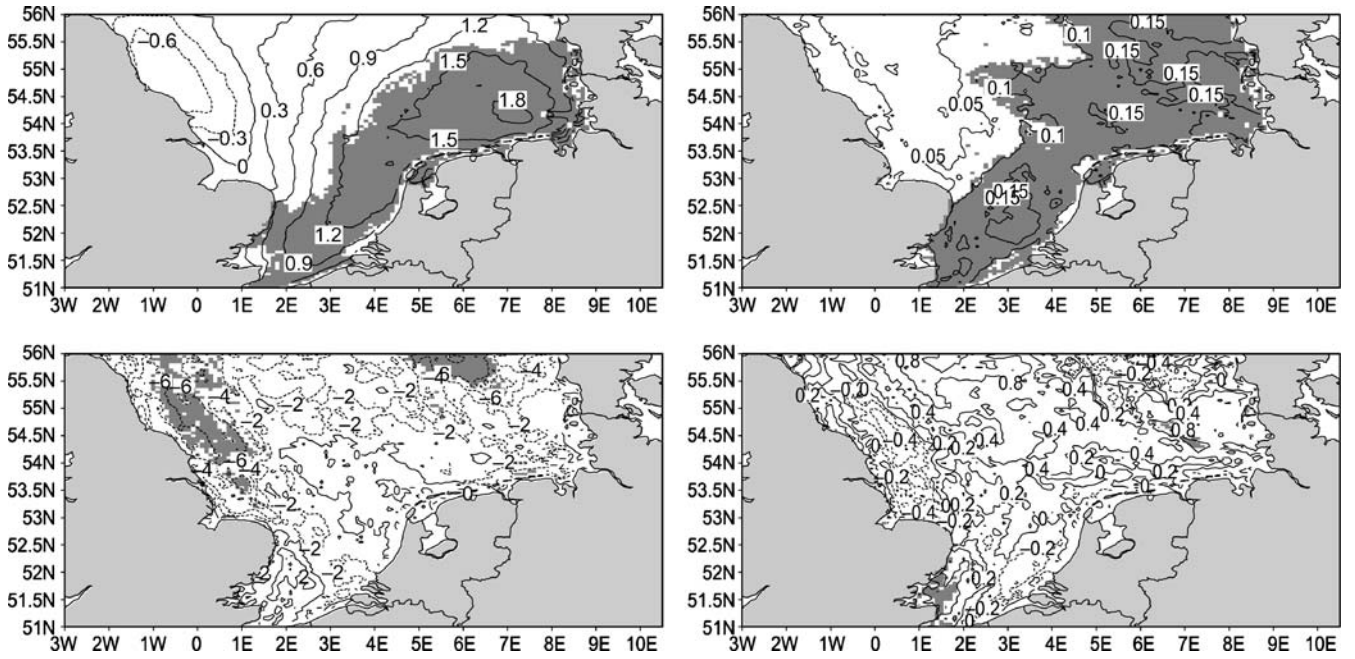


Fig. 7 Linear trends 1958–2002 of annual 99%-ile significant wave height in cm year^{-1} (upper left), of average annual number of events above SET in year^{-1} (upper right), of average duration of extreme events in min year^{-1} (lower left), and of average intensity of

extreme events in cm year^{-1} (lower right). Areas for which the trends are statistically different from zero at the 95% significance level are indicated by dark gray shading

indices for Northwest Europe (Alexandersson et al. 1998, 2000), it is known that storm activity in the area has been relatively weak around 1960 with a noticeable increase afterward until around 1990–1995. Later, storm activity has decreased again. From the analysis of wind data used to force our model with, a similar behavior has been found. Here, the average number of storms per year has increased near the exit of the North Atlantic Storm track and over the Southern North Sea since the beginning of the simulation period (1958), but the increase has attenuated later over the North Sea, and the average number of storms per year is decreasing over the Northeast Atlantic since about 1990–1995 (Weisse et al. 2005). To analyze whether a similar behavior is also found for the statistics of extreme wave events, we follow the strategy of Weisse et al. (2005) and slightly increased the complexity of the previously applied linear trend model

$$y_i = ax_i + b, \quad (1)$$

where y_i denotes any extreme wave event characteristic in year i , x denotes time, and a the linear trend. Following Weisse et al. (2005), the model (Eq. 1) was modified such that trends may change their amplitude and/or sign *once* at any year T during the 1958–2002 hindcast period

$$a, b = \begin{cases} a_1, b_1 & : i \leq T \\ a_2, b_2 & : i > T \end{cases} \quad (2)$$

with the continuity condition

$$a_1 x_T + b_1 = a_2 x_T + b_2 \quad (3)$$

The results of this slightly more complex linear trend model will be referred to as *piecewise linear trends*. Note that the year T at which trends may change their amplitudes and/or sign also represents a free parameter that is fitted to the data. For each grid point, it provides a rough indication at which year within the hindcast period trends most likely may have changed. The piecewise linear trend model was fitted to the data locally at each grid point using a least square method.

Note that this slightly more complex model is not intended to provide the best possible fit to the data but to investigate whether or not the simple linear trends (Fig. 7) can be considered as representative for the entire 1958–2002 period. For simplicity, the analysis is limited to the local annual 99%-ile significant wave height.

The result of this analysis is shown in Fig. 8. It can be inferred that the area east of about 2–4°E is characterized by a rather uniform pattern. Here, the period before 1990/1995 was characterized by rather strong increases of about 2–3 cm year^{-1} in annual 99%-ile wave heights. After about 1990/1995, the same area was characterized by decreases in extreme wave heights in the order of 1–6 cm year^{-1} depending on area.

The skill of the piecewise relative to the linear trend model was assessed using the Brier skill score defined by (von Storch and Zwiers 1999)

$$B = 1 - \sigma_F^2 \sigma_R^{-2}, \quad (4)$$

where σ_F^2 and σ_R^2 represent the error variances of the “forecast” F (here provided by the piecewise linear trend model) and the reference “forecast” R (here the simpler

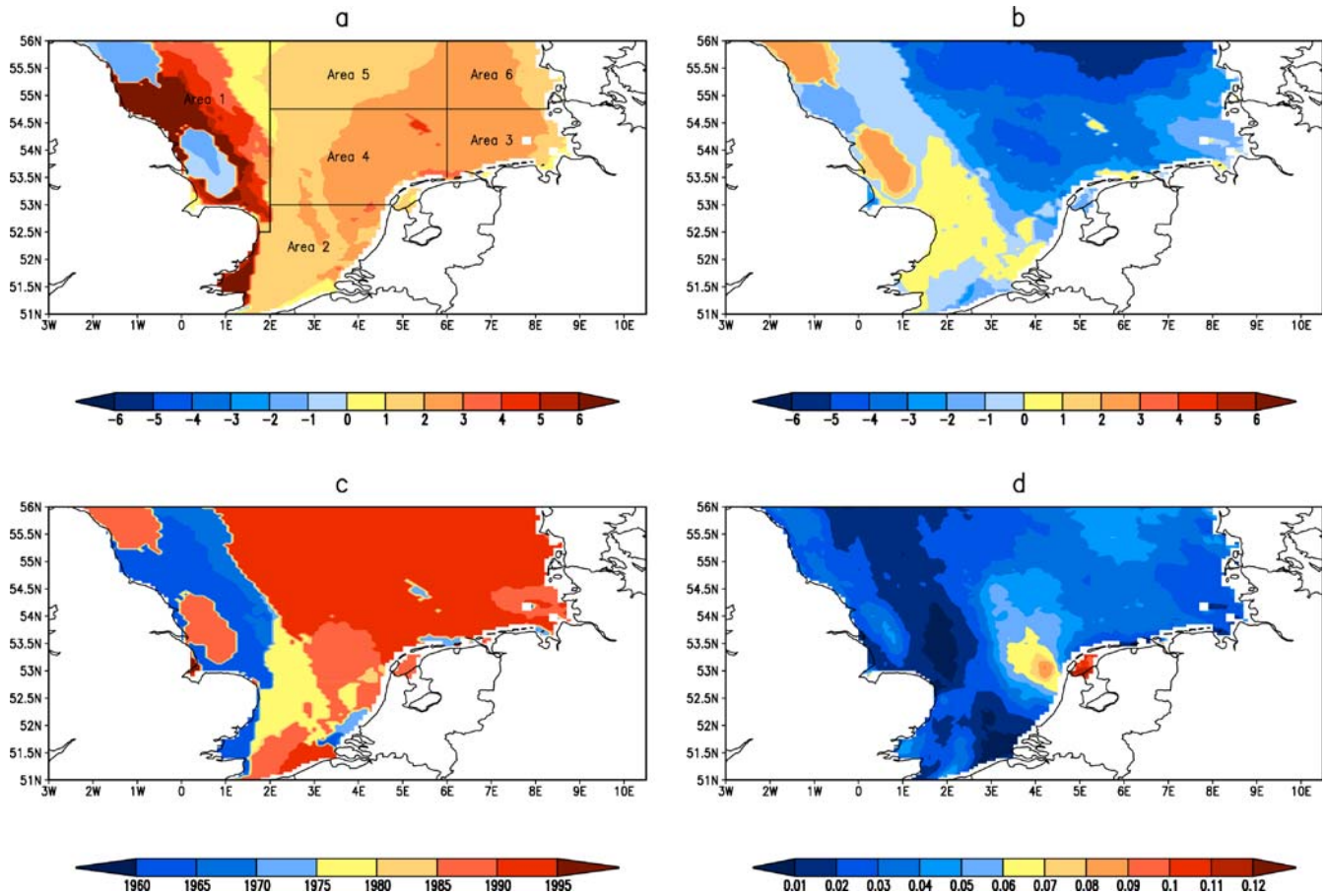


Fig. 8 Piecewise linear trends of annual 99%-ile significant wave heights. **a** Linear trend a_1 for the period 1958– T , **b** linear trend a_2 for the period T –2001. Units in both cases are cm year^{-1} . **c** Year T

at which a change in trends is indicated by the statistical model. **d** Skill of the piecewise linear trend model relative to the simple linear trend model. For exact definitions, see text

time independent linear trend model). The error variances are computed relative to the same predictand, here the gridded hindcast annual 99%-ile significant wave heights in 1958–2002.

In this analysis, the Brier score provides a measure of the skill of the piecewise linear model relative to the simple linear time independent model. Any positive value of B indicates that the piecewise linear trend model fits the data better than the time independent linear trend model. Negative values would indicate a better performance of the reference. However, in our case, the Brier score cannot be smaller than zero. If the time independent trend model would fit the data perfectly, the piecewise linear trend model would degenerate to $a_1 = a_2$ and $b_1 = b_2$ resulting in a Brier score of $B = 0$ as the smallest possible value. In our case, the Brier score may thus be interpreted the following way: It may reach values between zero and one, measuring the improvement in fitting the data obtained from the piecewise linear trend model in percent relative to the time independent linear trend model. The more the Brier score is different from zero, the larger is the improvement obtained from the piecewise linear model and the more inappropriate it is to assess changes in

extreme wave conditions from linear trends fitted over the period 1958–2002. The result of this exercise is shown in Fig. 8d. It can be obtained that the Brier score is non-zero everywhere. However, for most regions, the improvement is relatively small and ranges between about 2 and 5% only.

To visualize the time behavior of the wave extremes in more detail, we have divided the model domain into six areas characterized by different long-term evolutions in their wave regime (Table 3). For these areas, spatially averaged time series of significant wave height were determined from which annual 99%-iles and exceedance statistics have been computed. For the German Bight (areas 3–6), the time series basically exhibit a similar pattern: Extreme wave heights have increased from the beginning of the simulation period until a maximum (in the running mean time series) between about 1990 and 1995 is reached. Afterward, a decrease in extreme wave heights seems to prevail. This long-term development can be decomposed into an increase of the frequency of severe wave events that has leveled off around 1985 and an attenuation in the intensity and the duration of these events, although more data after 2002 are needed to fully assess the significance in the change of the extreme wave height trends. The behavior

Table 3 Definition of areas for which area averaged time series have been computed

Number	Description	Area
1	UK coast	North of 52.50°N West of 02.00°E
2	Southwestern North Sea	South of 53.00°N
3	Inner German Bight	53.00–54.75°N East of 06.00°E
4	Outer German Bight I	53.00–54.75°N 02.00–06.00°E
5	Outer German Bight II	54.75–56.00°N 02.00–06.00°E
6	Outer German Bight III	54.75–56.00°N east of 06.00°E

The areas are also indicated in Fig. 8a.

is shown exemplarily for area 3 in Fig. 9. However, as the development for the number of severe wave events closely corresponds to that reported for the number of storms in the area (Weisse et al. 2005) and the evolution of the annual wave height 99%-iles parallels that described for percentile based North Sea storm indices derived from pressure observations (Alexandersson et al. 2000), it may remain

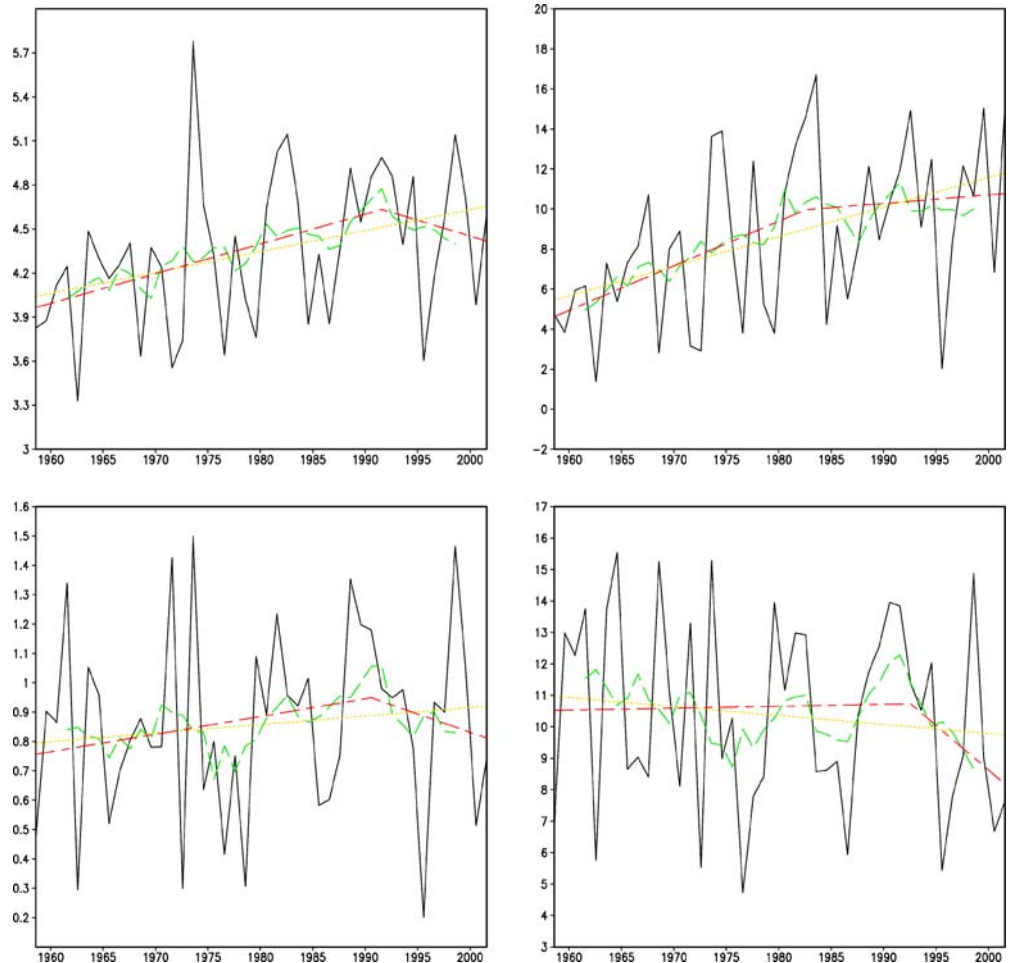
likely that the attenuation of severe wave events has continued until now as an update of the storm indices reveals decreasing storm activities until 2005 (von Storch, 2005, personal communication).

For the UK coast and the Southwestern North Sea, somewhat different patterns are obtained: Whereas there is hardly any noticeable change except for a slight and non-significant decreasing trend along the UK coast, for the Southwestern North Sea, an increase in extreme wave conditions is found that is most pronounced at the beginning of the hindcast period and which has leveled off later (not shown).

6 Summary and discussion

Long-term changes in extreme wave conditions are difficult to detect and to analyze because of the rare occurrence of these events as well as their limited spatial and temporal extend. Analyses of long-term changes require long and homogeneous time series that cover the area of interest at high spatial and temporal detail, a requirement that is frequently not fulfilled by the available observational data. Wave hindcasts with numerical models have therefore become a common tool to complement existing observations and to analyze trends and variability

Fig. 9 Inner German Bight: Time series of annual 99%-iles of significant wave height in m (*upper left*), annual number of events exceeding the SET (*upper right*), their average intensity in m (*lower left*), and their average duration in h (*lower right*). Time series from annual values (*black*), 7-year running means (*green*), linear trend (*yellow*), and piecewise linear trends (*red*)



of severe wave events (e.g., Günther et al. 1998; Sterl et al. 1998; Wang and Swail 2002).

So far, most of the existing wave hindcasts are limited either in their regional detail or in the length of period for which they have been performed. In addition, the quality and the homogeneity of the driving wind fields remain an issue. In this study, a high-resolution wave hindcast for the Southern North Sea covering the past 45 years has been presented. The wave hindcast was driven by high-resolution wind fields obtained from a regional atmosphere model (Feser et al. 2001; Weisse et al. 2005) forced by the NCEP/NCAR weather reanalysis (Kalnay et al. 1996; Kistler et al. 2001). In the latter, inhomogeneities caused by changes in analysis or data assimilation techniques have been reduced to a minimum. Although of course little can be done to improve the quality, coverage, and the resolution of the observational data used in the reanalysis, inhomogeneities related to changing analysis techniques are strongly reduced by using fixed state-of-the-art numerical models and data assimilation techniques. Hodges et al. (2003) and Bromwich et al. (2007) compared storm statistics in different global reanalyses and also analyzed the impact of major changes in the observational system. For Northern Hemisphere storms, they found little difference between the different reanalysis products and only small impacts due to changes in the observational system. On multi-decadal time scales, the global reanalyses therefore presently represent the best homogeneous products available so far. Because of that, we expected that our wave hindcast also represent one of the most homogeneous and longest high-resolution wave data sets available for the Southern North Sea so far. Data from this hindcast are available hourly for the past 45 years and are expected to be more suitable for the analysis of extreme wave events.

A comparison of hindcast and observations indicates that the hindcast reasonably simulates the North Sea wave climate of the past few decades. The conclusion holds for both mean and extreme value statistics. In particular, it was shown that simple statistics such as bias, root-mean-square error and correlation indicate a good agreement between measurements and simulation and that extreme value statistics at stations located seaward of about 10–15 m water depth are reproduced within error bounds. For stations surrounded by complex shallow topographic features not resolved in the hindcasts, an overestimation of the most severe wave conditions was found. Gaslikova and Weisse (2006) showed, however, that for these locations the wave hindcast presented in this paper nevertheless provides a good source for boundary conditions for very shallow water wave modeling and that a better representation of near-shore wave conditions can be obtained when further downscaling is applied. Therefore, it is suggested that the multi-decadal wave hindcast for the Southern North Sea is suitable for analyzing extreme value statistics seaward of about 10–15 m water depth, whereas toward the coast additional downscaling is required.

The analysis of long-term changes in extreme wave events reveals an increase in 99%-ile significant wave heights for much of the Southern North Sea within the past decades. For much of the area, this change is composed of an increase in total significant wave height followed by a subsequent decrease in the last few years. For much of the area, the initial increase in 99%-ile wave heights is mainly caused by an increase of the number of extreme wave events, whereas their duration and intensity remained nearly unchanged. Later, the increase of the number of extreme events leveled off, whereas duration and intensity of the events show an indication toward smaller values resulting in a decrease in 99%-ile significant wave heights.

The long-term changes in severe wave height conditions closely follow and correspond to that of storminess in the area. In 1998, the WASA group analyzed changes in the storm climate over the Northeast North Atlantic based on various sources. They concluded that although pronounced variability is present in the data sets, no clear long-term change could be identified. Instead, they state that storm climate has indeed roughened in the past decades but that the present storm climate (in 1995) is comparable to that at the beginning of the century (The WASA-Group 1998). The conclusion was mainly supported by a study of (Alexandersson et al. 1998) who analyzed upper intra-annual percentiles of geostrophic wind speed derived from station pressure data. Updates of this analysis reveal that storm activity has further decreased in the area within the last few years (Alexandersson et al. 2000; von Storch, 2005, personal communication).

The time evolution of the percentile-based storm indices from Alexandersson et al. (2000) thus closely follows that described for the 99%-ile significant wave height in the Southern North Sea. Closer inspection of the wave height changes revealed that this change could be viewed as being composed of an upward trend in the number of severe wave events at the beginning of the hindcast period that leveled off later and a decrease in the duration and intensity of extreme wave events. The temporal development of the number of severe wave events is in accordance with that described for the number of storms by Weisse et al. (2005) who analyzed long-term changes in storminess within the regional atmosphere model data used to force our wave model with.

To summarize, we conclude that ocean wave heights and their extremes are reasonably well simulated in our multi-decadal high-resolution wave hindcast for the Southern North Sea. This enables us to analyze long-term changes of extreme wave conditions. The latter indicate that for much of the area, 99%-ile wave heights have increased until about 1990–1995 and decreased afterward. It is, however, open whether the downward trends in wave heights and storminess will continue within the coming years or whether a reinforcement of storm activity and related severe wave events will occur.

Acknowledgment We thank Frauke Feser for providing us with the high-resolution wind fields to force our wave model with. Magnar Reistad from the Norwegian Meteorological Institute kindly provided us with sea ice data used as boundary conditions in the model simulation. A bathymetry for the Southern North Sea was obtained from the Bundesanstalt für Wasserbau. Observational data used for the model validation have been provided by Koos Doekes from Rijkswaterstaat and the Koninklijk Nederlands Meteorologisch Instituut (HYDRA project). We are grateful to Mrs. Gardeike for assistance with the graphics. This work has been financially supported by funding from the European Union under the HIPOCAS project (contract EVK2-CT-1999-00038).

References

- Alexandersson H, Schmith T, Iden K, Tuomenvirta H (1998) Long-term variations of the storm climate over NW Europe. *Global Atmos Ocean Syst* 6:97–120
- Alexandersson H, Tuomenvirta H, Schmith T, Iden K (2000) Trends of storms in NW Europe derived from an updated pressure data set. *Climate Res* 14:71–73
- Bromwich D, Fogt R, Hodges K, Walsh J (2007) Tropospheric assessment of ERA-40, NCEP, and JRA-25 global reanalyses in the polar regions. *J Geophys Res* (in press)
- Caires S, Sterl A (2005) 100-year return value estimates for ocean wind speed and significant wave height from the ERA-40 data. *J Climate* 18:1032–1048
- Cardone V, Jensen R, Resio T, Swail V, Cox A (1996) Evaluation of contemporary ocean wave models in rare extreme events: the “Halloween Storm” of October 1991 and the “Storm of the Century” of March 1993. *J Atmos Ocean Technol* 13:198–230
- Cox A, Swail V (2001) A global wave hindcast over the period 1958–1997: validation and climate assessment. *J Geophys Res* 106:2313–2329
- Ewing J, Weare T, Worthington B (1979) Hindcast study of extreme wave conditions in the North Sea. *J Geophys Res* 84:5739–5747
- Feser F, Weisse R, von Storch H (2001) Multi-decadal atmospheric modeling for Europe yields multi-purpose data. *Eos Transactions* 82:305, 310
- Gaslikova L, Weisse R (2006) Estimating near-shore wave statistics from regional hindcasts using downscaling techniques. *Ocean Dynamics* 56:26–35
- Günther H, Rosenthal W, Stawarz M, Carretero J, Gomez M, Lozano I, Serrano O, Reistad M (1998) The wave climate of the Northeast Atlantic over the period 1955–1994: the WASA wave hindcast. *Global Atmos Ocean Syst* 6:121–164
- Hodges K, Hoskins B, Boyle J, Thorncroft C (2003) A comparison of recent reanalysis datasets using objective feature tracking: storm tracks and tropical easterly waves. *Mon Weather Rev* 131:2012–2037
- Jacob D, Podzun R (1997) Sensitivity studies with the regional climate model REMO. *Meteorol Atmos Phys* 63:119–129
- Kalnay E, Kanamitsu M, Kistler R, Collins W, Deaven D, Gandin L, Iredell M, Saha S, White G, Woollen J, Zhu Y, Chelliah M, Ebisuzaki W, Higgins W, Janowiak J, Mo K, Ropelewski C, Wang J, Leetmaa A, Reynolds R, Jenne R, Joseph D (1996) The NCEP/NCAR reanalysis project. *Bull Am Meteorol Soc* 77:437–471
- Kistler R, Kalnay E, Collins W, Saha S, White G, Wollen J, Chelliah M, Ebisuzaki W, Kanamitsu M, Kousky V, van den Dool H, Jenne R, Fioriono M (2001) The NCEP/NCAR 50-year reanalysis: monthly means CD-ROM and documentation. *Bull Am Meteorol Soc* 82:247–267
- Meinke I, von Storch H, Feser F (2004) A validation of the cloud parameterization in the regional model SN-REMO. *J Geophys Res* 109:D13205
- OSPAR Commission (2000) Quality status report 2000, region II Greater North Sea OSPAR Commission, London, pp 136+xiii
- Soares C, Weisse R, Carretero J, Alvarez E (2002) A 40 years hindcast of wind, sea level and waves in European waters. In: Proc. 21st international conference on offshore mechanics and arctic engineering, Norway, Oslo, 23–28 June 2002
- Sterl A, Caires S (2005) Climatology, variability and extrema of ocean waves-The web-based KNMI/ERA-40 wave atlas. *Int J Climatol* 25:963–977
- Sterl A, Komen G, Cotton P (1998) Fifteen years of global wave hindcasts using winds from the European Centre for Medium-Range Weather Forecasts reanalysis: validating the reanalyzed winds and assessing wave climate. *J Geophys Res* 103:5477–5492
- The WAMDI-Group (1988) The WAM model—a third generation ocean wave prediction model. *J Phys Oceanogr* 18:1776–1810
- The WASA-Group (1998) Changing waves and storms in the Northeast Atlantic? *Bull Am Meteorol Soc* 79:741–760
- von Storch H, Zwiers FW (1999) Statistical analysis in climate research. Cambridge University Press, New York, p 494
- von Storch H, Langenberg H, Feser F (2000) A spectral nudging technique for dynamical downscaling purposes. *Mon Weather Rev* 128:3664–3673
- Wang X, Swail V (2002) Trends of atlantic wave extremes as simulated in a 40-yr wave hindcast using kinematically reanalyzed wind fields. *J Climate* 15:1020–1035
- Weisse R, Feser F (2003) Evaluation of a method to reduce uncertainty in wind hindcasts performed with regional atmosphere models. *Coast Eng* 48:211–225
- Weisse R, Pluess A (2006) Storm-related sea level variations along the North Sea coast as simulated by a high-resolution model 1958–2002. *Ocean Dynamics* 56:16–25
- Weisse R, Feser F, Günther H (2003) Wind-und Seegangsklimatologie 1958–2001 für die südliche Nordsee basierend auf Modellrechnungen GKSS Report 2003/10 GKSS Forschungszentrum Geesthacht GmbH Max-Planck-Str. 1, D-21502 Geesthacht, Germany, p 38
- Weisse R, von Storch H, Feser F (2005) Northeast Atlantic and North Sea storminess as simulated by a regional climate model 1958–2001 and comparison with observations. *J Climate* 18:465–479